

## Influence of Hydrothermal-carbonization Process on Biochar Properties from Cattail Weed Waste

Araya Smuthkochorn<sup>1</sup>, Nardnutda Katunyoo<sup>1</sup>, Napat Kaewtrakulchai<sup>1</sup>,  
Duangduen Atong<sup>2</sup>, Kanit Soongprasit<sup>2</sup>, Masayoshi Fuji<sup>3</sup> and Apiluck Eiad-ua<sup>1\*</sup>

<sup>1</sup>College of Nanotechnology, King Mongkut's Institute of Technology Ladkrabang,  
Bangkok, Thailand

<sup>2</sup>National Metal and Materials Technology Center (MTEC), Bangkok, Thailand

<sup>3</sup>Advanced Ceramic Research Center, Nagoya Institute of Technology,  
Tajimi, Japan

Received: 9 May 2018, Revised: 20 November 2018, Accepted: 29 January 2019

### Abstract

Biochars have been successfully synthesized from Cattail leave (CL) via hydrothermal and carbonization process. The experimental work described has focused on physical properties of biochars produced from Cattail leaves at 160, 180 and 200°C for 8, 12 and 24 h for hydrothermal and substituted to carbonization at 700°C for 2 h. The influences of hydrothermal and carbonization on the pore structure, surface functional groups and the product yield was also investigated by characterization using Scanning Electron Microscope (SEM) and Fourier Transform Infrared Spectroscopy, respectively. Although the morphologies of cell structures were maintained in the hydrothermal and carbonization, it was found that the yield of produced biochar was decreased with increase of the hydrothermal temperature and time. The images from SEM showed that the pore structures are quite roughness on their external surface of biochar and the functional group of their surface area has most of pure carbon content (59-65 wt%).

**Keywords:** Cattail leaves, Carbonization, Hydrothermal, Biochar  
DOI 10.14456/cast.2019.2

### 1. Introduction

A wide range types of biomass have been utilized for energy, conversion options, end-use applications and infrastructure requirements [1]. Biomass is derived from agriculture waste such as coconut shell, palm shell, rice straw, coffee ground, etc. [2-3], harvesting forestry and other plant residues. The biomass feedstocks have been collected, transported and possibly stored, before being processed into a suitable form for energy conversion technology [4-5]. The energy produced from used of biomass is only one of renewable energy that can reduce the impact of energy production, in which there are many ways to minimize such effects as a GHG emissions.

---

\*Corresponding author: Tel.: +66 (0)2329 8000 Ext. 3132 Fax: +66 (0) 2329 8265  
E-mail: apiluck.ei@kmitl.ac.th

Cattail wetland plants are weed found in all area throughout Thailand, generally grow and spread vigorously under the right conditions through their root systems and seed. The seeds germinate rapidly under hot, moist conditions and can be ready for transplant in just a few months, which gives the main cause of the flooding and spoiling. Cattail leaves can be used as the cheapest source for energy production, carbon sequestration, and as an essential element for the production of hydrochars and active carbons [6]. In the past few years, the conversion of biomass waste into valuable carbon materials has received considerable attention due to the ability to produce hydrochars with attractive characteristics that promote efficiency for a variety of applications [7-12] such as supporting materials for environment, energy technology and improvement of bio-oil properties [13].

Traditionally, carbonization is a thermochemical conversion process that can be applied for the development of biomass to carbon materials. On the other hand, hydrothermal-carbonization is the technique to modify chemical structure using water for conversion of biomass to carbon products which gives higher yield than carbonization [14-17]. Most organic matters in raw materials for feedstocks are transformed into solid, depending on the temperature and time via hydrothermal-carbonization process. The formation of biochar from lignin materials via direct solid conversion of biomass formation [18] and polymerization or condensation monomer generated from decomposition of biomass are proposed [19].

In this study biochar was prepared from Cattail leaves by hydrothermal and carbonization process. The produced biochars were characterized by Scanning Electron Microscope, Elemental Analyzer and Fourier Transform Infrared Spectroscopy. This research work aims to study the effects of hydrothermal-carbonization temperatures and times on the pore structure, elemental contents, surface functional groups and yields of resulting product. The potential applications of biochar derived cattail leaves as an alternative energy were also examined.

## 2. Materials and Methods

### 2.1 Preparation of raw material

Lignocellulosic biomass from Cattail leaves (CL)(*Typha angustifolia* Linn.) was used as raw material for producing biochar. Cattail is generally a weed that can be found in all areas throughout Thailand. Cattail leaves biomass were dried at 110°C for 24 h to remove moisture, then crushing into smaller size using a knife mill.

### 2.2 Hydrothermal-carbonization of Cattail leaves

Regarding biochar production, 20 grams of CL biomass were mixed with 400 ml of deionization water and then reformulated with hydrothermal at 160, 180 and 200°C for 8, 12 and 24 h in stainless-steel chamber. Then, the samples were carbonized at 700°C under nitrogen flow in stainless-steel reactor for 1 h by a ramp rate at 10°C/min. All experimental conditions for biochar derived from CL were shown in Table 1. The resulting biochar produced at 160, 180 and 200°C for 8, 12 and 24 h was labeled as CL-160-8, CL-160-12, CL-160-24, CL-180-8, CL-180-12, CL-180-24, CL-200-8, CL-200-12 and CL-200-24, respectively.

**Table 1.** Conditions of biochar derived from Cattail leaves.

Sample	Temperature (°C)	Time (h.)
CL-160-8	160	8
CL-160-12	160	12
CL-160-24	160	24
CL-180-8	180	8
CL-180-12	180	12
CL-180-24	180	24
CL-200-8	200	8
CL-200-12	200	12
CL-200-24	200	24

### 2.3 Characterization of biochar derived from Cattail leaves

The production yield of biochar was calculated with applied formula as follows:

$$Y (\%) = m/m_0 \times 100$$

Where Y is the yield (%) of produced biochar, m is mass of produced biochar (g), and  $m_0$  is raw cattail leaves biomass (g).

In order to observe the pore structure, elemental contents and surface morphologies of CL derived biochar with different hydrothermal-carbonization conditions, these samples were examined using high-resolution scanning electron microscopy (SEM, Zeiss EVO MA 10). Due to the chemical compositions of biochar products rich in lignocellulosic components, the elemental analysis of resulting materials was conducted using an elemental analyzer (Elementar, Vario EL III) in terms of carbon (C), hydrogen (H) and nitrogen (N) wt%. The surface functional groups of biochar were analyzed by Fourier-Transform Infrared Spectroscopy (FT-IR, Perkin Elmer Spectrum). The spectra were performed between 4000-400  $\text{cm}^{-1}$  to observe the influences of hydrothermal-carbonization conditions on the efficiency of carbon conversion to the biochar products.

## 3. Results and Discussion

### 3.1 Yield of biochar products

The thermal decomposition of biochar during hydrothermal-carbonization experiment produced three products including solid char, condensable liquid and non-condensable gas, the relative amounts of three products depend on experimental conditions. The yield of biochar is defined as the ratio of the weight of biochar after carbonization to the weight of the raw materials as seen from the applied formula in previously reported [20]. On the other hand, the hydrothermal temperature and time play an important role in the yield (%) of biochar. As seen from Figure 1 the yield of resulting biochar products decreased, this is due to the loss of volatile materials with increasing hydrothermal-carbonization temperature and time. It should be noted that the yield (%) of the resulting biochar prepared at a specific hydrothermal temperature for the hydrothermal time of 24 h (CL-160-24, CL-180-24 and CL-200-24 was about 43.04, 41.77 and 47.29% respectively)

was higher than the hydrothermal time (8 and 12 h), the presence of time promotes the re-polymerization [21] of constituent biopolymer, hydrothermal sample is influenced by hydrolysis which is the determining first step that exhibits water soluble organic compounds. The solid product is subsequently formed by re-condensation reaction of soluble organic compounds in water, resulting in the increased yield of biochar. The availability of the fragments from hydrolysis in the liquid phase offers a huge potential to influence product characteristics due to the excessive duration of holding time during hydrothermal carbonization.

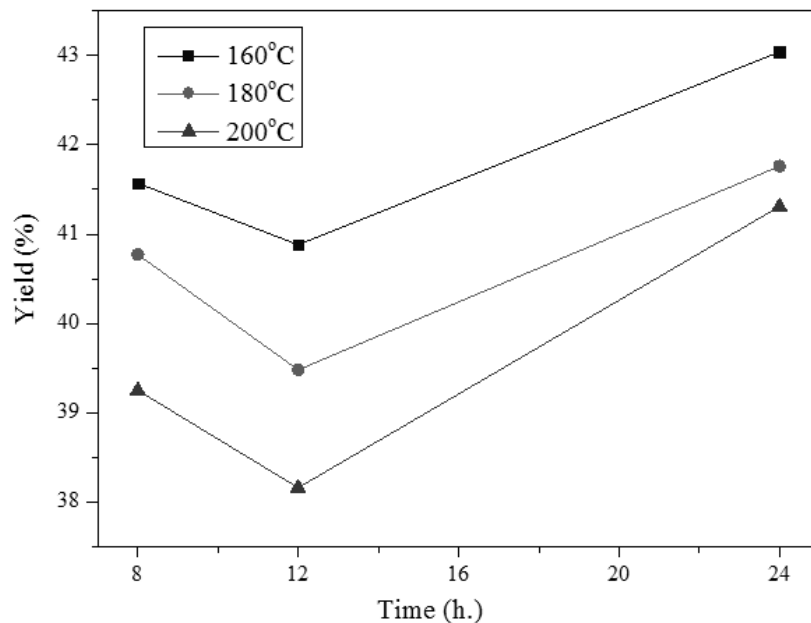


**Figure 1.** The effect of hydrothermal-carbonization temperature and time on the yield of biochar products.

### 3.2 Morphology of the resulting biochar products under SEM observation

Scanning Electron Microscope (SEM) measurements were performed using SEM Zeiss EVO MA10 operated at 10 kV to observe the surface morphology and pore structure of resulting biochar products derived from Cattail leaves biomass. Figure 2 (a-i) shows SEM image of biochar hydrothermal-carbonization at 160, 180 and 200°C for 8, 12 and 24 h, respectively. The biochar sample displayed a much rougher and irregular surface textures when the temperature and time of the hydrothermal-carbonization increased. However, at the highest hydrothermal time (24 h), the pore structure was changed due to heat shrinkage as shown in Figure 2 (c), (f), (i). A various cavity on their surface resulted from the thermal decomposition of lignocellulosic polymer (i.e. cellulose, hemicellulose and lignin). Under the experimental conditions, a hydrothermal temperature of 200°C for 12 h as seen in Figure 2 (f) was found to be the optimization of pore structure for desired biochar product.

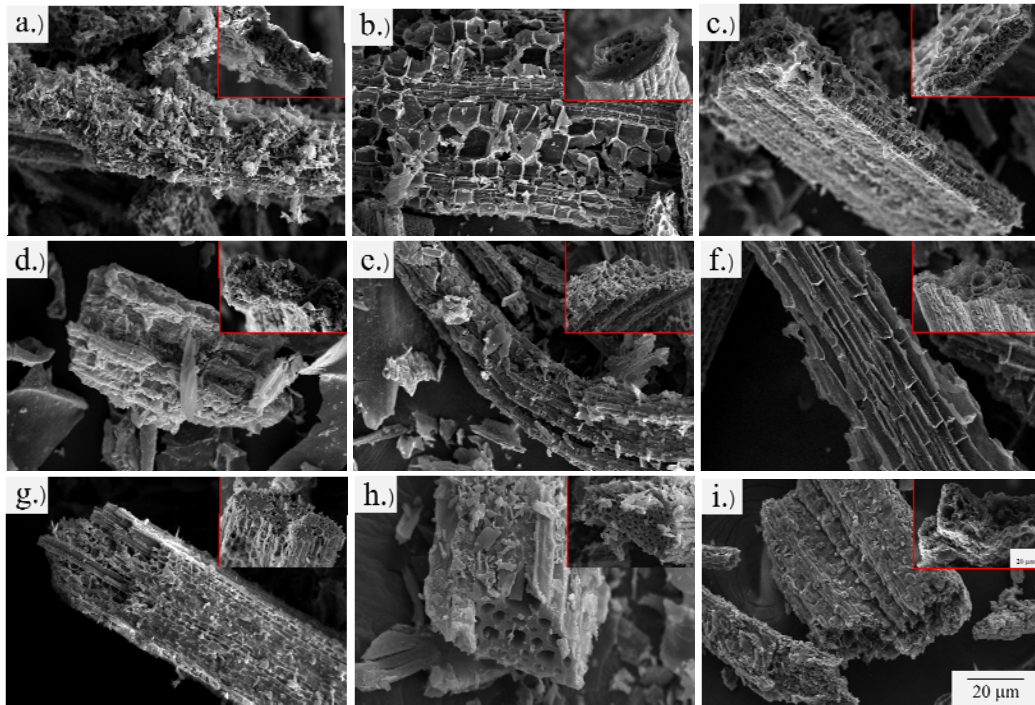


**Figure 2.** SEM images (300X, 500X) of biochar products from hydrothermal-carbonization at (a) 160°C-8 h. (b) 160°C-12 h. (c) 160°C-24 h. (d) 180°C-8 h. (e) 180°C-12 h. (f) 180°C-24 h. (g) 200°C-8 h. (h) 200°C-12 h. (i) 200°C-24 h.

### 3.3 Elemental analyses of biochar products

The results of CHN contents are shown in Table 2. The analysis was done by using elemental composition of HTC products. Obviously, these products were rich in carbon contents, which should be derived from lignocellulosic materials as Cattail leaves biomass. The carbon contents in the biochars were around 59-65 wt%, thus resulting in relatively high carbon contents. It should be noted that the hydrogen contents of resulting biochars at specific hydrothermal-carbonization temperature for the hydrothermal time at 24 h were higher than at 12 and 8 h, which could be attributable to the efficiencies of carbon at the long hydrothermal holding time. In contrast, the carbonization process could create more percentage of carbon content. In comparison, the elemental contents of a typical carbon product used in alternative application such as carbon sorbent (activated carbons) was found to be more percentage of carbon content (above 70%). More interestingly, an increase in the textural pore characteristic of biochar products is associated with increasing hydrothermal-carbonization temperature and holding time. Carbon content (%) was also increased while hydrogen and nitrogen contents were decreased.

**Table 2.** Elemental contents of biochar products

Sample	C (wt%)	H (wt%)	N (wt%)
CL-160-8	61.720	0.762	1.390
CL-160-12	63.931	0.175	1.501
CL-160-24	60.613	0.705	1.408
CL-180-8	61.406	0.792	1.635
CL-180-12	61.566	0.730	1.433
CL-180-24	64.411	0.127	1.829
CL-200-8	59.521	0.474	1.867
CL-200-12	60.516	0.685	1.794
CL-200-24	60.987	0.724	1.844

### 3.4 Functional group of biochar products

The carbon matrix does not consist of carbon atoms alone, but is bonded with any atoms like oxygen, hydrogen and nitrogen, etc. These govern the surface chemistry of the biochar products [22]. Infrared spectroscopy provides the functional group on the surface area of products and depending on the precursor and the synthesis steps. The bands of biochar observed in Figure 3 after hydrothermal-carbonization were characterized by using Fourier-Transform Infrared Spectroscopy (FT-IR, Perkin Elmer Spectrum). Considering the FTIR spectra of the biochars as described by Lu *et al.* [23] with the bands covering similar or the same wavelength as observed for the investigated carbon, the FTIR spectra of biochar derived from Cattail leaves also show strong bands at 1000-930  $\text{cm}^{-1}$  due to the C-O and C=C stretching vibrations which was related to cellulose and hemicellulose usually found in any plants. The bands at 1600  $\text{cm}^{-1}$  are due to vibration mode of C-O stretching and are designated as the lignin group. The bands at 2920  $\text{cm}^{-1}$ , C-H stretching are also designated as the lignin group. The region from 3420-2840  $\text{cm}^{-1}$  represents the O-H stretching vibrations and is designated as the surface functional group in hydroxyl group and water. Moreover, the bonding of carbon to the other atoms contained in the raw materials such as nitrogen, oxygen and hydrogen is found. These are the bonds of organic compounds in the biomass and after hydrothermal carbonization the bonding of these compounds is destroyed due to the hydrolysis from water and thermal cracking from thermal treatment, resulting in the peaks of the FTIR spectrum. The intensity of the compounds such as C-N is extremely low and cannot be observed in the FTIR results.

FTIR spectra of biochar products with different hydrothermal temperatures and times are illustrated in Figure 3 and percentages of surface functional group that appeared on the surface of resulting materials (calculated by integrated information obtained from the graph) are represented in Figure 4. By considering the percentage of functional group with an increasing hydrothermal temperature, a number of change was found in the bands approximately at 1000-930, 1600 and 2920  $\text{cm}^{-1}$  with the presence of carbon vibrations around 2-30%. It could be explained that there was the transformation of organic compounds to carbons. The relative intensity of the bands at approximately 3420-2840  $\text{cm}^{-1}$  decreases about 10% when compared to their intensity of Cattail leaves precursor, which is resulted from the evaporation of water molecules during the process. However, it can be noticed that all carbons are observed at the bands of 1600 and 2920 (Figure 3). The bands between around 1000-930  $\text{cm}^{-1}$  have often been observed for carbons and carbonaceous materials [24]. The increased temperature and carbonization holding time also exhibits more releasing of volatile substances and represented as high purity of carbon product.

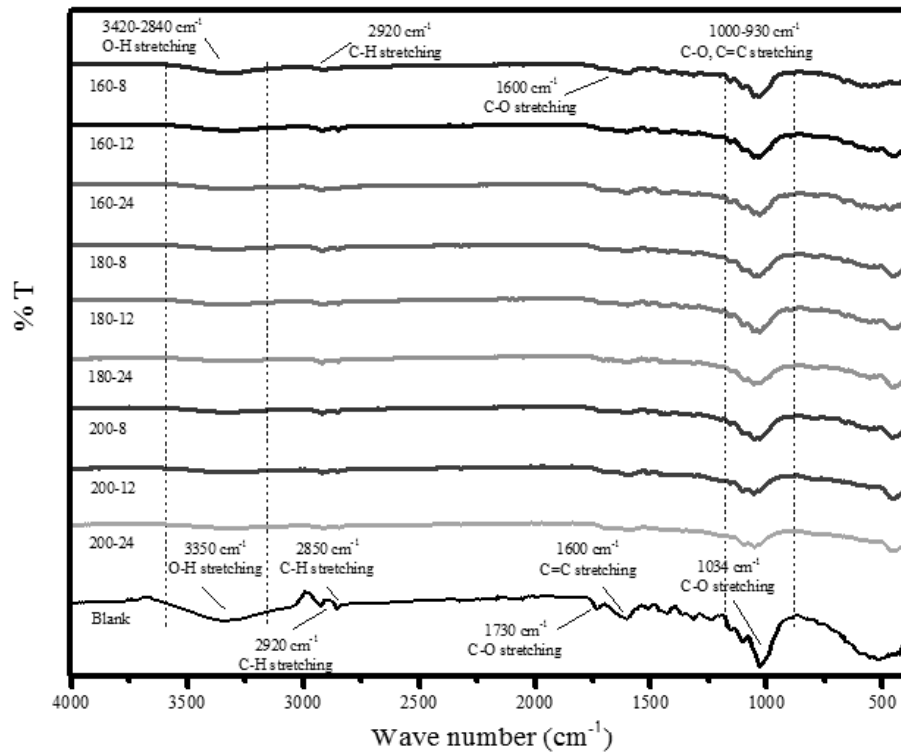


**Figure 3.** FTIR spectra of the biochar products prepared by hydrothermal-carbonization at different temperatures and times.

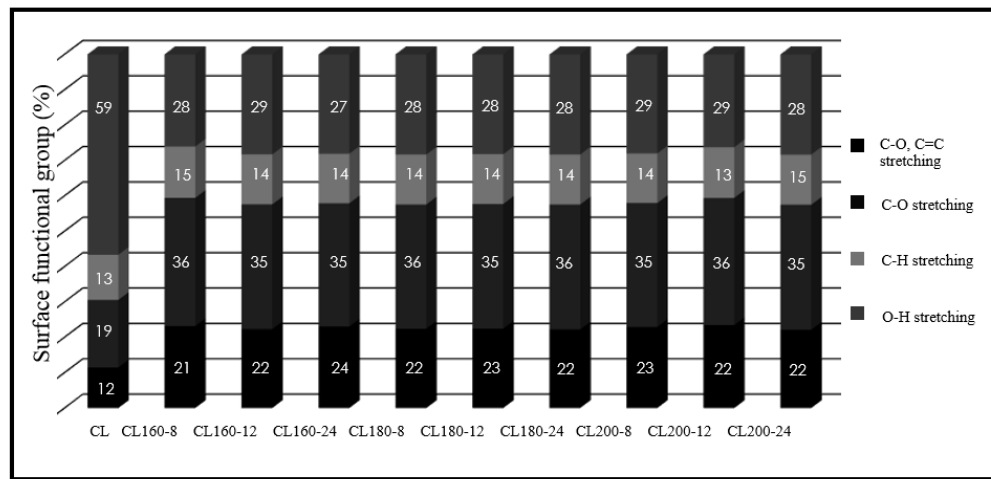


**Figure 4.** Percentages of the surface functional group of the biochar products prepared by hydrothermal-carbonization at different temperatures and times.

#### 4. Conclusions

This study represents high potential of biochars prepared from Cattail leaves biomass via hydrothermal-carbonization process. Hydrothermal temperature significantly affects the pore development, elemental contents and surface functional group of biochars. The yields of resulting products produced by hydrothermal-carbonization process are higher than only carbonization process. The pore properties of resulting materials and carbon conversion efficiencies are increased. More interestingly, the resulting biochars have significant carbon contents of 59-65 wt%, with lower nitrogen and hydrogen contents. Further study should be investigated on conversion of biomass to be used as alternative energy.

#### 5. Acknowledgements

The authors would like to thank the College of Nanotechnology, King Mongkut's Institute of Technology Ladkrabang (KMITL), Bangkok, Thailand and the financial support of the National Metal and Materials Technology Center (MTEC) via the YSTP program of National Science and Technology Development Agency (NSTDA), Pathumthani, Thailand (Grant GNA-CO-2560-4662-TH/2560) for their supports.

#### References

- [1] Devid, P., Scoot, H., 1986. *Market Assessment of Biomass Gasification and Combustion Technology for Small- and Medium-Scale Applications*: A national laboratory of the U.S. Department of Energy.
- [2] Satya Sai, P.M., Ahmed, J., 1997. Production of activated carbon from coconut shell char in a fluidized bed reactor. *Industrial and Engineering Chemistry Research*, 36 (9), 3625-3630.
- [3] Donni, A., Wan, M., Mohd, K., 2005. Preparation and characterization of activated carbon from palm shell by chemical activation with  $K_2CO_3$ . *Bioresorce Technology*, 98, 145-149.
- [4] Peter, M., 2001. Energy production from biomass (part 2) conversion technology. *Bioresorce Technology*, 83, 47-54.
- [5] Kacem, M., Pellerano, M., 2015. Pressure swing adsorption for  $CO_2/N_2$  and  $CO_2/CH_4$  separation: comparison between activated carbons and zeolites performances. *Fuel Process Technology*, 138, 271-283.
- [6] Liu, Z., Zhang, F.S., 2009. Removal of lead from water using biochars prepared from hydrothermal liquefaction of biomass. *Journal of Hazardous Materials*, 167, 933-939.
- [7] Liu, Z., Zhang, F.S., 2010. Characterization and application of chars produced from pinewood pyrolysis and hydrothermal treatment. *Fuel*, 89, 510-514.
- [8] Selvi, B.R., Jagadeesan, D., Suma, B., Nagashaniar, G., Arif, M., Balasubramanyam, K., Eswaramoorthy, M., Khudu, T.K., 2003. Intrinsically fluorescent carbon nanosphere as a nuclear targeting vector: delivery of membrane-impermeable molecule to modulate gene expression in vivo. *Nano Letters*, 8(10), 3182-3188.
- [9] Titirici, M., Antonietti, M., Thomas, A., 2006. A generalized synthesis of metal oxide hollow spheres using hydrothermal approach. *Chemistry of Materials*, 18(16), 3808-3812.
- [10] Sevilla, M., Fuertes, A., Mokaya, R., 2011. High density hydrogen storage in superactivated carbons from hydrothermally carbonized renewable organic materials. *Energy and Environmental Science*, 4, 1400-1410.

- [11] Sevilla, M., Fuertes, A.B., 2011. A superior performance for carbon dioxide capture. *Energy and Environmental Science*, 4, 1765-1771.
- [12] Faisal, A., Sahu, J.N., 2011. Optimization and characterization studies on bio-oil production from palm shell by pyrolysis using response surface methodology. *Biomass and Bioenergy*, 35, 3604-3616.
- [13] Chao, C., Wha-Seung, A., 2011. CO<sub>2</sub> capture using mesoporous alumina prepared by a sol-gel process. *Chemical Engineering Journal*, 166, 646-651.
- [14] Sevilla, M., Macia-Agollo, J.A., Fuerest, A.B., 2011. Hydrothermal carbonization of biomass as a route for the sequestration of carbon dioxide chemical and structural properties of the carbonized products. *Biomass and Bioenergy*, 33, 3152-3159.
- [15] Kamimura, Y., Shimomura, M., Endo, A., 2016. CO<sub>2</sub> adsorption-desorption properties of zeolite beta prepared from OSDA-free synthesis. *Microporous and Mesoporous Materials*, 219, 125-133.
- [16] Jarosław, S., Urszula, N., Antoni, W.M., Rafał, J.W., Beata, M., 2017. Highly microporous activated carbons from biomass for CO<sub>2</sub> capture and effective micropores at different conditions. *Journal of CO<sub>2</sub> Utilization*, 18, 73–79.
- [17] Berge, N.D., Ro, K.S., Mao, J., Flora, J.R.V., Chappell M.A., Bae, S., 2011. Hydrothermal carbonization of municipal waste streams. *Environmental. Science and Technology*, 45(13), 5696-5703.
- [18] Minkova, V., Razvigorova, M., Goranova, M., Ljutzen, L., Angelona, G., 1991. Effect of water vapor on the pyrolysis of solid fuel. *Fuel*, 71, 263-265.
- [19] Gergova, K., Galushko, A., Petrov, N., Minkova, V., 1992. Investigation of the porous structure of activated carbons prepared by pyrolysis of agricultural by-products in a stream of water vapour. *Biomass and Bioenergy*, 30, 721-730.
- [20] Dilek, A., 2013. Effect of pyrolysis temperature and heating rate on biochar obtained from pyrolysis of safflower seed press cake. *Bioresource Technology*, 128, 593-597.
- [21] Ayillath, K., Paresh, L., 2015. Lignin depolymerization into aromatic monomer over solid acid catalysts. *ACS Catalysis*, 5(1), 365-379.
- [22] Solum, M.S., Pugmire, R.J., Jagtoyen, M., Derbyshire, F., 1995. Evolution of carbon structure in chemically activated wood. *Carbon*, 33, 1247-1254.
- [23] Lu, C., Bai, H., Wu, B., Su, F., Hwang, J.F., 2008. Adsorption of Carbon Dioxide from Gas Streams via Mesoporous Spherical-Silica Particles. *Energy and Fuels*, 489-496.
- [24] Serafin, J., Narkiewicz, U., Morawski, A.W., Wróbel, R.J., Michalkiewicz, B., 2017. Standing out the key role of ultramicroporosity to tailor biomass-derived carbons for CO<sub>2</sub> capture. *Journal of CO<sub>2</sub> Utilization*, 230, 73-79.